Diagnostic and Interventional Imaging (2015) **96**, 477—486

View metadata, citation and similar papers at core.ac.uk

brought to you by CORE

provided by Elsevier - Publisher Connector

ORIGINAL ARTICLE /*Research and innovation*

Dose reduction with iterative reconstruction: Optimization of CT protocols in clinical practice

J. Greffier [a,*], F. Macri [a], A. Larbi [a], A. Fernandez [a], E. Khasanova [a,b], F. Pereira [a], C. Mekkaoui [a,c], J.P. Beregi [a]

[a] *Department of Radiology, University Hospital Center of Nîmes, EA 2415, Bd Prof Robert-Debré, 30029 Nîmes cedex, France*
[b] *Dana-Farber Cancer Institute, Harvard Medical School, Boston, USA*
[c] *Harvard Medical School, Massachusetts General Hospital, Department of Radiology, Martinos Center for Biomedical Imaging, Boston, USA*

KEYWORDS
Multidetector CT;
Iterative reconstruction;
Dose reduction;
Image quality;
Patient safety

Abstract
Objectives: To create an adaptable and global approach for optimizing MDCT protocols by evaluating the influence of acquisition parameters and Iterative Reconstruction (IR) on dose reduction and image quality.
Materials and methods: MDCT acquisitions were performed on quality image phantom by varying kVp, mAs, and pitch for the same collimation. The raw data were reconstructed by FBP and Sinogram Affirmed Iterative Reconstruction (SAFIRE) with different reconstruction kernel and thickness. A total of 4032 combinations of parameters were obtained. Indices of quality image (image noise, NCT, CNR, SNR, NPS and MTF) were analyzed. We developed a software in order to facilitate the optimization between dose reduction and image quality. Its outcomes were verified on an adult anthropomorphic phantom.
Results: Dose reduction resulted in the increase of image noise and the decrease of SNR and CNR. The use of IR improved these indices for the same dose without affecting NCT and MTF.

Abbreviations: CNR, Contrast-to-Noise Ratio; CTDI, Computed Tomography Dose Index; DRL, Diagnostic Reference Levels; FBP, Filtered Back Projection; FOV, Field-Of-View; IR, Iterative Reconstruction; LDPE, Low-Density PolyEthylene; LSF, Line Spread Function; MDCT, Multi-Detector Computed Tomography; MTF, Modulation Transfer Function; NCT, CT Number; NPS, Noise Power Spectrum; PSF, Point Spread Function; ROI, Region Of Interest; SAFIRE, Sinogram Affirmed Iterative Reconstruction; SNR, Signal-to-Noise Ratio; VBA, Visual Basic Application.

* Corresponding author. CHU de Nîmes, Bd Prof Robert-Debré, 30029 Nîmes Cedex 9, France.
E-mail address: joel.greffier@chu-nimes.fr (J. Greffier).

http://dx.doi.org/10.1016/j.diii.2015.02.007
2211-5684/© 2015 Éditions françaises de radiologie. Published by Elsevier Masson SAS. All rights reserved.

The image validation was performed by the anthropomorphic phantom. The software proposed combinations of parameters to reduce doses while keeping indices of the image quality adequate. We observed a CTDIvol reduction between −44% and −83% as compared to the French diagnostic reference levels (DRL) for different anatomical localization.
Conclusion: The software developed in this study may help radiologists in selecting adequate combinations of parameters that allows to obtain an appropriate image with dose reduction.

© 2015 Éditions françaises de radiologie. Published by Elsevier Masson SAS. All rights reserved.

Introduction

Due to a growing demand of computed tomography (CT) examinations, patients are being exposed more frequently to ionizing radiation [1]. To address this increasing medical/clinical requirement, health care professionals are asked to strengthen the rationale for examinations and to optimize practices and procedures. The optimization is achieved by simultaneously managing the dose level and the image quality [2,3]. Changes in the parameters of the image acquisitions can be arranged to reduce the dose delivered to patients but this causes a deterioration of the image quality [4].

Recent advances in iterative reconstruction (IR) methods of MDCT images have provided a reliable and alternative method for optimizing the ratio between the dose and the image quality. These methods consist in post-processing mathematical approaches that allow us to correct raw data by reducing image noise without changing the transverse spatial resolution [5,6]. Several studies have demonstrated that it is possible to maintain satisfactory image quality with dose reduction [7—19]. However, the dose reduction is usually a medical judgment and the gain in the image quality obtained by IR needs to be quantified. Those studies evaluated intra-group comparison with optionally chosen acquisition and reconstruction parameters. Moreover, dosimetric and qualitative analyses were made a posteriori.

The purpose of this work was to define an adaptable and global approach for optimizing MDCT protocols by evaluating the influence of acquisition parameters, SAFIRE on dose reduction and image quality by using the phantom Catphan 500 and an anthropomorphic phantom. We developed a software in order to facilitate the optimization between dose reduction and image quality.

Materials and methods

MDCT protocol

Images were acquired on a MDCT SOMATOM Definition AS + (Siemens, Erlangen, Germany) with floating diaphragm on the 3 axes allowing to obtain a collimation of 128×0.6 mm from an array of 64 detectors 0.6 mm. Raw data were reconstructed using two procedures: Filtered Back Projection (FBP) and Sinogram Affirmed Iterative Reconstruction (SAFIRE). The latter uses two corrections loops, which are applied on the raw data and on the image data with five iteration levels (S1 to S5) respectively [16,20].

Phantom Quality Image

A Catphan 500 phantom (The Phantom Laboratory, Salem, USA) was used to assess the quality of image based on the acquisition parameter and the levels of SAFIRE. Three sections of the phantom (CTP 401, CTP 486 and CTP 528a) were studied. The CTP 401 section is composed of four inserts of distinct densities. Each section aims to assess both signal (CT Number (NCT)) and image noise in the Air (−1000 HU), in Low-Density PolyEthylene (LDPE, −100 HU), in Acrylic (120 HU) and in Teflon (950 HU).

The CTP 486 section consists of a uniform section for measuring NCT and image noise of a material that owns density close to the water, (20 HU). Finally, the CTP 528a section is used to assess the transverse spatial resolution by the computing the Modulation Transfer Function (MTF).

Standardized method for acquisition and reconstruction parameters

Raw data were collected and reconstructed according to the parameters presented in Table 1. These parameters are available on the MCDT and include five levels of iteration in SAFIRE (S1 to S5). Overall, 4032 combinations of parameters were obtained.

Dosimetry

For each acquisition Computerized Tomography Dose Index volume (CTDIvol) was measured with the dosimetry phantom body (The Phantom Laboratory, Salem, USA) with 32 cm of diameter and a pencil ionization chamber of 10 cm. The ionization chamber and the multimeter were calibrated according to an accredited laboratory (Swedish Board for Conformity Assessment and Accreditation 2035 ISO/IEC/17025).

Physical metrics

Except for Noise Power Spectrum (NSP), data were analyzed with the CTP module software Qualimagiq (QUALIFORMED,

Table 1 Parameter of Acquisition and Reconstruction studied: in total, 4032 combinations of parameters are available.

	Parameters used in the software	Parameters presented in the paper
kVp	80, 100, 120, 140	80, 100, 120
mAs	50, 100, 150, 200, 250, 300, 350	50, 100, 150, 200
Pitch	0.8, 1.2	0,8
Kernel	B/I30f, B/I40f, B/I50f, B/I70f	B/I30f
Thickness/Overlap	1 mm/0.7 mm; 2 mm/1 mm; 3 mm/1 mm	1 mm/0.7 mm
Reconstruction Type	FBP, S1, S2, S3, S4, S5	FBP, S1, S2, S3, S4, S5

La Roche sur Yon, France). NCT (mean of pixel values in regions of interest) and image noise (standard Deviation of pixel values in regions of interest) were estimated on the CTP 401 sensitometric section and on the CTP 486 uniform section. Measurements on the CTP 401 section were carried out in the center of the four inserts (Air, LDPE, Acrylic and Teflon) with regions of interest (ROI) of 420 pixels (0.785 cm^2). The NCT and the image noise of the water on the CTP 486 section were assessed by placing a ROI of 14,400 pixels (36 cm^2) in the center of the phantom representing 40% of its diameter. In order to obtain accurate results, the NCT and image noise were assessed out on 10 consecutive sections and described as average with a standard deviation from the mean.

From the values on these two sections, the signal-to-noise ratio (SNR) and the contrast-to-noise ratio (CNR) [21] were calculated according the Equation (1) and (2) respectively. The CNR was obtained by considering the image noise values and the water NCT as a reference in the Equation (2).

$$SNR = \left| \frac{HU_{ROI}}{\sigma_{ROI}} \right| \quad (1)$$

$$CNR = \frac{|HU_{ROI} - HU_{Water}|}{\frac{(\sigma_{ROI}+\sigma_{Water})}{2}} \quad (2)$$

The transverse spatial resolution, characterized by the MTF [22–24], was calculated by measuring the impulse response function of the imaging system represented by the spreading function of a point also known as ''Point Spread Function (PSF)''. This function was estimated in the 528 bis CTP section, composed of a small ball of Tungsten Carbide with diameter of 0.28 mm, which is less than one pixel in size. A square area of 32 pixels was centered on the middle of the PSF (maximum intensity pixel) and the background signal was subtracted therein.

To reduce the influence of noise, two spread functions of a line source (Line Spread Function: LSF) were calculated by projecting the different PSF profiles depending on vertical and horizontal directions of the image. At the end, the MTF was obtained from the average of 2 modules of the Fourier transform of 2 LSFs. Image noise properties can be characterized by the noise power spectrum (NPS). It measures, depending on the frequency, the noise component and the image smoothing with the dose reduction and the use of SAFIRE. NPS were calculated with a home-made Matlab® routine (The MathWorks, Natick, USA) based on 60 image slices of the homogeneous water section (CTP 486) containing ROIs of 128 × 128 pixels. NPS were determined by averages in the frequency domain along the fx and fy directions [21,25–28].

Proposal of software for data analysis

We developed a macro in Excel (Microsoft, Redmont, USA) using Visual Basic for Applications (VBA) from the 4032 available parameters. This software was applied on the database with distinct acquisition and reconstruction parameters in combination with values of CTDIvol, MTF10%, image noise, SNR and CNR.

The usage of the software is done within three steps. First, the operator chooses acquisition and reconstruction parameters present on the workstation (Table 1). Second, the operator elects the distinct parameters to be kept for the output; for example, the same kVp, the same reconstruction type or the same reconstruction kernel used in the first step. As a final step, the operator defines the minimum percentage of dose reduction and maximum variation of image quality indices (image noise, SNR, CNR, MTF10%). Only the combination of parameters with the image quality indices that were not reduced more than 5% compared to the reference acquisition was retained. In this study, a standard sequence was chosen to illustrate the optimization possibilities offered by this software. As first step, the sequence studied was performed with 120 kVp, 200 mAs and FBP as reference. Pitch 0.8 and for collimation was in 128 × 0.6 mm. The raw data were reconstructed with slice thickness of 1 mm every 0.7 mm, by Filtered Back Projection with a reconstruction kernel ''Medium Smooth'' B30f. Then, the same kVp, pitch, collimation, slice thickness and reconstruction kernel were entered in addition to levels of SAFIRE (S1, S2, S3, S4, S5). Finally, we choose a minimal dose reduction of 20% that did not impair image quality indices.

Data verification on anthropomorphic phantom

Post-process data were verified on an adult anthropomorphic phantom ''ATOM Dosimetry Phantoms'' (CIRS, Norfolk, USA). Comparisons of image noise, CNR and SNR were performed by positioning ROI in structures having densities similar to those of the phantom Catphan 500 inserts: Air (0.004*10^{23} cm^{-3}) vs. Lung tissue (0.681*10^{23} cm^{-3}); Water (3.343 *10^{23} cm^{-3}) vs. Soft tissue (3.434 *10^{23} cm^{-3}) and Teflon (6.243*10^{23} cm^{-3}) vs. Bone tissue (5.028*10^{23} cm^{-3}). No comparison was possible between the two phantoms for LDPE and acrylic.

Optimization in clinical practice

The MDCT protocols were optimized by using the parameters combinations proposed by the software and after validation

with anthropomorphic phantom. Several combinations of parameters were offered according anatomical location: Head, Abdomen-Pelvic, Chest, Chest-Abdomen-Pelvic and Lumbar Spine. The quality of the phantom images for each proposed combinations were accepted by radiologists of our department.

The impact of the aforementioned technique was assessed by means of the comparison of news CTDIvol with the French Diagnostic Reference levels (DRL) [29] and CTDIvol before optimization. These CTDIvol corresponded to the mean of CTDIvol obtained during one year on all CT exams on two CT scan (same brand) in our department.

Statistics

Statistical analysis was performed using 'Biostatgv' (http://marne.u707.jussieu.fr/biostatgv). The comparison for Catphan 500 phantom between the reference acquisition and other acquisitions was obtained using the paired Mann Whitney-Wilcoxon test. A P-value < 0.005 (adjusted for multiple comparisons) was considered significant.

Results

Physical metrics

Changes in kVp resulted in significant variation ($P < 0.005$) of the NCT as shown in Table 2a, independently of the inserts location. For example, the water NCT were 12.1 HU for 120kVp, 2.6 HU for 100 kVp and −13.2 HU for 80 kVp. Unlikely, reduction of the number of mAs or the increases of the level of SAFIRE did not cause significant ($P > 0.005$) changes on the NCT. Compared to the reference (120 kVp, 200 mAs and FBP), reduction in kVp or in mAs values were associated with increasing noise in the image (Table 2b). Compared to the reference acquisition with 80 kVp and 200 mAs water image noise was increased by 78% and 31% with 120kVp and 100 mAs, respectively. Significant noise reduction ($P < 0.005$) was observed when higher levels of SAFIRE were applied. Compared to the reference acquisition water image noise was decreased by −19% with S1, −37% with S3 and −55% with S5. Regarding the FBP, the image noise reduction was more pronounced in LDPE, Water and Acrylic (−50% to −60% between FBP and S5) than Air or Teflon (−19% to −21% between FBP and S5).

The degradation of CNR due to reductions of kVp was observed according to the variation of NCT and to the increment of image noise (Table 2c). For example, the Acrylic CNR were 11.5 for 120kVp, 9.8 for 100 kVp and 6.2 for 80 kVp. The degradation of CNR due to mAs reduction was also noticed with significant increase in image noise ($P < 0.005$). The acrylic CNR for 120 kVp was 11.5, 8.2 and 5.8 with 200, 100 and 50 mAs, respectively. Along with application of higher level of SAFIRE, the CNR was improved for all inserts. Compared to the reference acquisition, the acrylic CNR was increased by 18% with S1, 57% with S3 and 133% with S5. Regarding the FBP, improvement of CNR was more pronounced in LDPE and Acrylic (51% to 53% between FBP and S5) than in air or Teflon (112% to 133% between FBP and S5).

Table 2a Effects of kVp, mAs and reconstruction type on CT number.

	CT Number (HU)				
	Air	LDPE	Water	Acrylic	Teflon
120 kVp 200 mAs FBP B30f	−1000.9	−90.7	12.1	122.0	940.5
100 kVp 200 mAs FBP B30f	−1000.8*	−100.6*	2.6*	115.3*	953.8*
80 kVp 200 mAs FBP B30f	−995.2*	−117.8*	−13.2*	101.3*	984.9*
120 kVp 150 mAs FBP B30f	−999.5	−87.5	12.0	123.3	940.2
120 kVp 100 mAs FBP B30f	−1000.1	−88.7	11.9	120.4	935.6
120 kVp 50 mAs FBP B30f	−995.4*	−91.3	11.8	122.6	936.2
120 kVp 200 mAs SAFIRE I30f S1	−1001.0	−90.7	12.1	122.1	940.6
120 kVp 200 mAs SAFIRE I30f S3	−1001.3	−91.0	12.1	122.0	941.0
120 kVp 200 mAs SAFIRE I30f S5	−1001.6	−91.1	12.1	122.0	941.3

Table 2b Effects of kVp, mAs and reconstruction type on Image Noise.

	Image Noise				
	Air	LDPE	Water	Acrylic	Teflon
120 kVp 200 mAs FBP B30f	14.1	8.0	9.9	9.2	14.4
100 kVp 200 mAs FBP B30f	14.9	10.9*	11.7*	11.4*	20.8*
80 kVp 200 mAs FBP B30f	19.0*	14.5*	17.6*	19.7*	22.5*
120 kVp 150 mAs FBP B30f	15.5	9.3*	10.6*	10.7*	15.9
120 kVp 100 mAs FBP B30f	16.0*	13.0*	13.0*	13.3*	17.4*
120 kVp 50 mAs FBP B30f	18.0*	18.2*	18.0*	20.4*	28.3*
120 kVp 200 mAs SAFIRE I30f S1	13.5 + (−4.3%)	7.1 + (−11.1%)	8.0 + (−19.1%)	8.1 + (−11.6%)	13.8 + (−3.9%)
120 kVp 200 mAs SAFIRE I30f S3	12.3 + (−12.6%)	5.4 + (−32.7%)	6.2 + (−37.2%)	5.9 + (−35.6%)	12.7 + (−11.5%)
120 kVp 200 mAs SAFIRE I30f S5	11.2 + (−20.7%)	4.0 + (−50.4%)	4.5 + (−54.5%)	3.7 + (−59.9%)	11.6 + (−19.1%)

Table 2c Effect of kVp, mAs and reconstruction type on CNR.

	Contrast-to-Noise Ratio			
	Air	LDPE	Acrylic	Teflon
120 kVp 200 mAs FBP B30f	84.2	11.4	11.5	76.4
100 kVp 200 mAs FBP B30f	75.6*	9.2*	9.8*	58.6*
80 kVp 200 mAs FBP B30f	53.7*	6.5*	6.2*	49.8*
120 kVp 150 mAs FBP B30f	77.6*	10.0*	10.5	70.1
120 kVp 100 mAs FBP B30f	69.8*	7.7	8.2	60.7*
120 kVp 50 mAs FBP B30f	56.0*	5.7	5.8*	39.9*
120 kVp 200 mAs SAFIRE I30f S1	94.0 + (11.6%)	13.6 + (18.5%)	13.6 + (18.4%)	85.0 + (11.3%)
120 kVp 200 mAs SAFIRE I30f S3	109.2 + (29.6%)	17.7 + (54.8%)	18.1 + (57.4%)	98.0 + (28.3%)
120 kVp 200 mAs SAFIRE I30f S5	129.1 + (52.3%)	24.3 + (112.3%)	26.8 + (133.3%)	115.1 + (50.7%)

Changes in kVp, mAs or SAFIRE's level did not alter the transverse spatial resolution, which is expressed in the MTF curves and shown in Table 2d.

The Frequency Distribution of Noise (expressed by NPS) indicated that the image noise was increased in two situations: (i) for decreasing values of kVp but conserving the mAs (Fig. 1a) and (ii), for reducing values of mAs at the same kVp (Fig. 1b).

Compared to FBP, higher levels of SAFIRE decreased NPS. Moreover, the peaks of the NPS curves were shifted to lower frequencies when SAFIRE was applied (Fig. 1c).

Verification on anthropomorphic phantom of the combinations parameters proposed by the software

Table 3 shows the combination of parameters of acquisition and reconstruction. Regarding such output combinations, the variations of dose, image noise and CNR are entered, the software taking into account the definition made by the operator. The SAFIRE level 5 was the only one proposed over 50% of dose reduction.

The software proposed five possibilities of dose reduction ranging from 25% to 50%. It also suggested three possible SAFIRE levels: S3, S4 and S5. Values of image noise, SNR and CNR were maintained or improved and the transverse spatial resolution (MTF10%) was not changed. Table 4 shows the values of image noise, SNR and CNR for images acquired on the anthropomorphic phantom from parameters combinations suggested by the software. These values for the three structures had the same magnitude as those of the air, Water and Teflon on the phantom Catphan 500. Variation of image noise, SNR and CNR of combinations proposed with respect to the acquisition reference were, with the exception of the bone, more marked on the anthropomorphic phantom than phantom Catphan 500. Similar to phantom Catphan 500, the effect of SAFIRE was greater for the Water than for the bone and air.

Fig. 2 shows the position of the three ROI placed in the anthropomorphic phantom according to the selected tissues at distinct levels doses; for instance, the dose reduction with FBP (2a) 25% with S3 (2b) and 50% with S5 (2c).

Optimization on clinical practice

Table 5 shows CTDIvol values obtained in 2012 and 2013, before and after optimization of the parameters for different anatomical locations. This table also includes a

Table 2d Effect of kVp, mAs and reconstruction type on MTF.

	Modulation Transfer Function	
	MTF50%	MTF10%
120 kVp 200 mAs FBP B30f	3.56	6.11
100 kVp 200 mAs FBP B30f	3.56	6.13
80 kVp 200 mAs FBP B30f	3.51	6.05
120 kVp 150 mAs FBP B30f	3.55	6.11
120 kVp 100 mAs FBP B30f	3.59	6.18
120 kVp 50 mAs FBP B30f	3.59	6.18
120 kVp 200 mAs SAFIRE I30f S1	3.56	6.12
120 kVp 200 mAs SAFIRE I30f S3	3.57	6.14
120 kVp 200 mAs SAFIRE I30f S5	3.57	6.15

Values expresses the effects of kVp, mAs and reconstruction type on CT number (2a), image noise (2b), CNR (2c) and MTF (2d). Comparisons with the reference acquisition defined as: 120 kVp, 200 mAs with FBP. Noise and NCT water is used to calculate the CNR, CNR water is not presented in the Table 2c. (FBP: Filtered Back Projection, LDPE: Low-Density PolyEthylene). Significance compared to the reference acquisition * $P < 0.005$ and + $P < 0.005$ (when value was improved).

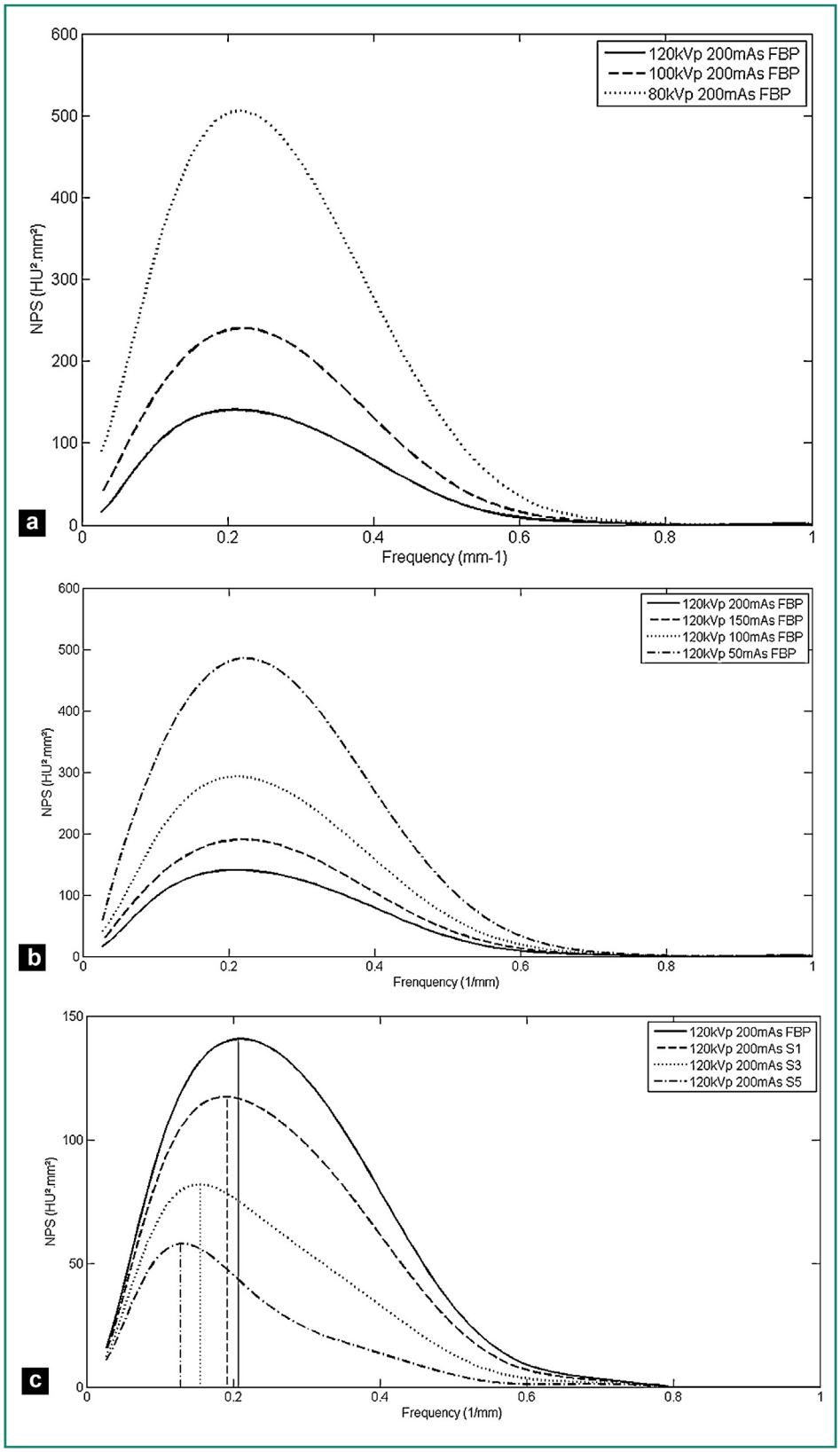

Figure 1. Noise Power Spectrum (NPS) curve for distinct kVp, mAs and reconstruction type. a. FBP (B30f), different kVp and 200 mAs. b. FBP (B30f) 120 kVp and different mAs. c. for 120 kVp and 200 mAs and FBP (B30f), S1, S3, S5 (I30f).

Table 3 Combinations of the parameters of acquisition and reconstruction.

			Air (El. density 0.004 10^{23} cm^{-3})			Water (El. density 3.343 10^{23} cm^{-3})		Teflon (El. density 6.243 10^{23} cm^{-3})		
CTDIvol (mGy)	mAs ref	Recon Type	Image Noise	SNR	CNR	Image Noise	SNR	Image Noise	SNR	CNR
13.4	200	FBP	14.1	70.9	84.2	8.9	1.4	14.4	65.4	76.4
10.1	150	S3	12.8	78.1	91.8+	7.4+	1.6	12.9	72.8	83.7+
10.1	150	S4	12.0+	83.3+	107.5+	6.4+	1.9+	12.0	77.9	100.4+
10.1	150	S5	11.0+	90.8	113.2	5.3+	2.2	11.2+	83.4+	102.3+
6.7	100	S4	13.6+	73.5+	93.4+	8.1+	1.5+	15.2	62.1	80.0
6.7	100	S5	12.9+	77.3	110.8+	6.9+	1.7	14.6	64.6	93.4+

The software works on 150 mAs (25% dose reduction) and uses levels SAFIRE S3 to S5 or 100 mAs (50% dose reduction) and S4 to S5. For 3 inserts (air, water, Teflon) values of noise, SNR and CNR, proposed by the tool combinations are close to or better than the values of the reference acquisition. (FBP: Filtered Back Projection, El: Electron, SNR: Signal-to-Noise Ratio, CNR: Contrast-to-Noise Ratio). Significance compared to the reference acquisition * $P < 0.005$ and + $P < 0.005$ (when value was improved).

Table 4 Verification with anthropomorphic phantom of combinations proposed by software.

			Lung tissue (El. density 0.681 10^{23} cm^{-3})			Soft tissue (El. density 3.434 10^{23} cm^{-3})		Bone tissue (El. density 5.028 10^{23} cm^{-3})		
CTDIvol (mGy)	mAs ref	Recon Type	Image Noise	SNR	CNR	Image Noise	SNR	Image Noise	SNR	CNR
13.4	200	FBP	11.0	72.2	81.6	9.0	2.4	14.0	57.9	68.5
10.1	150	S3	10.0	79.9	96.6	7.0	3.1	13.0	62.2	78.7
10.1	150	S4	9.0	88.8	109.5	6.0	3.7	12.0	67.4	87.4
10.1	150	S5	8.0	99.9	136.8	4.0	5.5	12.0	67.4	98.4
6.7	100	S4	10.0	79.7	96.5	7.0	3.3	15.0	54.1	71.7
6.7	100	S5	9.0	88.6	109.3	6.0	3.8	14.0	58.0	78.9

Noise, SNR and CNR were measured in Lung tissue, Soft tissue and Bone tissue on the anthropomorphic phantom for combinations proposed by the software. (FBP: Filtered Back Projection, El: Electron, SNR: Signal-to-Noise Ratio, CNR: Contrast-to-Noise Ratio). Significance compared to the reference acquisition * $P < 0.005$ and + $P < 0.005$ (when value was improved).

Figure 2. Images obtained from the three combinations defined, with values of SNR and CNR close to dose reductions of 25% and 50%. The same image settings were used for images a, b and c. a. 120 kVp; 200 mAs; FBP; CTDIvol: 13.5 mGy. b. 120 kVp; 150 mAs; S3; CTDIvol: 10.1 mGy. c. 120 kVp; 100 mAs; S5; CTDIvol: 6.7 mGy.

comparison with French DRL. After optimization, CTDIvol were reduced by 26% for the head, 32% for abdomen-pelvic, chest 40%, 35% for the chest-abdomen-pelvic and 55% for the lumbar spine. The same values measured in 2013 were between −44% and −83% below the French DRL.

Discussion

This experimental study used the phantom image quality Catphan 500 that allowed one to establish a database of 4032 combinations of acquisition and reconstruction

Table 5 CTDIvol values before and after implementation of an optimization approach, compared to French NRD.

CTDIvol (mGy)	Head	Abdomen-Pelvic	Chest	Chest Abdomen-Pelvic	Lumbar Spine
Nîmes 2012	48.8	7.5	4.2	10.2	36.3
Nîmes 2013	36.3	5.1	2.5	6.6	16.5
French NRD	65	17	15	20	45
% Difference (2013 vs. NRD)	−44	−70	−83	−67	−63
% Difference (2013 vs. 2012)	−26	−32	−40	−35	−55

The values expressed the CTDIvol obtained for five sequences before and after the implementation of an optimization and use of it tools approach. A comparison was made with the French NRD. The percentage difference between the values obtained in 2013 and 2012 or NRD was presented.

parameters with values CTDIvol, image noise, SNR, CNR and MTF10%.

The present software considered the influence of acquisition and reconstruction parameters on the dose and on image quality and allowed users to reduce the dose without impairing the image quality. Several studies [21,24,27] have focused on iterative reconstructions with the dose reduction associated to image quality by means of image quality phantoms. Decreases in mAs and kVp resulted in deterioration of the image quality indices together with increases in image noise and NPS, as well as deterioration of the SNR and CNR [21,24,27]. Thus, changes of kVp caused change in the NCT of distinct structures.

The present study supports previous literature [21,24,27] and confirms that SAFIRE change neither the transverse spatial resolution nor the NCT, independently of the inserts densities. Decreases of the image noise were observed when the levels of SAFIRE were increased as opposed to FBP. The impact of SAFIRE was less pronounced in structures with a high NCT e.g. air or Teflon. The values of image noise reduction from one level to another for Water were the same as those described in the literature [21,24,27]. This reduction of image noise resulted in increased SNR and CNR independently of the insert used.

The study of NPS between the FBP and the different levels of SAFIRE confirmed the noise reduction but exposed a shift of the curves peak toward to lower frequencies with increasing levels SAFIRE. In addition, the increase of levels of SAFIRE determined an increase of image smoothing [24,28].

Taking into account the influence of distinct acquisition and reconstruction parameters, we choose to reduce the doses by decreasing the mAs reference without changing the kVp. Compensation of degradation of image quality indices, especially those due to noise increase, was mainly assured by increasing levels of SAFIRE.

With the present study we were able to provide a rigorous and reproducible approach aiming to optimise the image quality settings from the established database. The ad-hoc implementation of the software gave the choice to operator to reduce the dose while keeping satisfactory quality image indices from the acquisition and reconstruction parameters. Given the large number of parameters analysed, this software has the advantage that it can be applied to the majority of the available protocols in the MDCT. As much as the dose reduction was defined by the operator, fewer combinations of parameters are available in the software.

Compensation was initially provided by SAFIRE. From the image quality point of view of, the use of increased levels of SAFIRE amplified the smoothing effect of the image with alteration of its texture. The shape of the NPS curves was modified and the peaks left-shifted toward the lower frequencies. The texture and quality of the phantom images were accepted by radiologists in our department for implementation in clinical routine. The verifications that were done on the anthropomorphic phantom for the combinations parameters proposed confirmed the efficacy of this software especially for soft tissues. Only the combination of parameters with the image quality indices that were not reduced more than 5% compared to the reference acquisition was retained.

The implementation of this tool in routine practice also seemed complex. With no direct synchronization of acquisition and reconstruction parameters on the MDCT workstation, the operator was obligated to manually enter the input and output parameters, the variations of the dose reduction and quality image indices. These last two points were physician-dependent and not always available at the workstation at same time.

Moreover, the software proposed here may be very useful for medical physicists for optimization approach of the parameters, because it constitutes a fair and substantial instrument of measures that takes into account all the parameters available on MDCT. In practice, all MDCT protocols of our reference center were optimized without deteriorating image quality. Reductions doses were obtained for the different anatomical locations with values well below French DRL [29]. The quality of images obtained with lower doses for all protocols was evaluated and considered as satisfactory by a radiologist and is conducted by a radiologist to evaluate satisfaction and efficacy.

This study has nevertheless some limitations. First, the Catphan device 500, used as reference to quantify the physical measures, was a quick and simple approach for the evaluation of certain properties of reconstruction methods and it was limited especially for MTF measurements with non-linear reconstruction. Second, even if the software database is composed of several values of pitch, reconstruction thickness and reconstruction kernels, the results presented in this study targeted the effect of SAFIRE, kVp and mAs on dose reduction and image quality. Third, the subjective quality criteria has not been studied. Finally, the impact of SAFIRE on the spatial resolution in the Z-axis was not studied either.

Conclusion

To conclude, the present work confirmed that the use of SAFIRE allows us to increase the quality of images with same dose or to keep adequate image quality with dose reduction. Also, using the software we developed helps to choose the dose reduction delivered to the patients in clinical practice.

Acknowledgements

We would like to thank R. Maingonnat for his help in this study; Mr C. Croisille, from Siemens France for his support on designing the study and helping with the discussion, and S. Beaumont for technical support with Qualimagiq software.

Disclosure of interest

The authors declare that they have no conflicts of interest concerning this article.

References

[1] Brenner DJ, Hall EJ. Computed tomography—an increasing source of radiation exposure. N Engl J Med 2007;357(22):2277—84.
[2] Kalra MK, Maher MM, Toth TL, Hamberg LM, Blake MA, Shepard JA, et al. Strategies for CT radiation dose optimization. Radiology 2004;230(3):619—28.
[3] Kalender WA, Buchenau S, Deak P, Kellermeier M, Langner O, van Straten M, et al. Technical approaches to the optimisation of CT. Phys Med 2008;24(2):71—9.
[4] Gunn ML, Kohr JR. State of the art: technologies for computed tomography dose reduction. Emerg Radiol 2010;17(3):209—18.
[5] Beister M, Kolditz D, Kalender WA. Iterative reconstruction methods in X-ray CT. Phys Med 2012;28(2):94—108.
[6] Kalender W, Computed Tomography:. Fundamentals, System Technology, Image Quality, Applications. Germany: Publicis; 2011. p. 111—74.
[7] Moscariello A, Takx RA, Schoepf UJ, Renker M, Zwerner PL, O'Brien TX, et al. Coronary CT angiography: image quality, diagnostic accuracy, and potential for radiation dose reduction using a novel iterative image reconstruction technique-comparison with traditional filtered back projection. Eur Radiol 2011;21(10):2130—8.
[8] Becce F, Ben Salah Y, Verdun FR, Van de Berg BC, Lecouvet FE, Meuli R, et al. Computed tomography of the cervical spine: comparison of image quality between a standard-dose and a low-dose protocol using filtered back-projection and iterative reconstruction. Skeletal Radiol 2013;42(7):937—45.
[9] Singh S, Kalra MK, Hsieh J, Licato PE, Do S, Pien HH, et al. Abdominal CT: Comparison of Adaptive Statistical Iterative and Filtered Back Projection Reconstruction Techniques. Radiology 2010;257(2):373—83.
[10] Yanagawa M, Honda O, Kikuyama A, Gyobu T, Sumikawa H, Koyama M, et al. Pulmonary nodules: effect of adaptive statistical iterative reconstruction (ASIR) technique on performance of a computer-aided detection (CAD) system-comparison of performance between different-dose CT scans. Eur J Radiol 2012;81(10):2877—86.
[11] Baker ME, Dong F, Primak A, Obuchowski NA, Einstein D, Gandhi N, et al. Contrast-to-noise ratio and low-contrast object resolution on full- and low-dose MDCT: SAFIRE versus filtered back projection in a low-contrast object phantom and in the liver. AJR Am J Roentgenol 2012;199(1):8—18.
[12] von Falck C, Bratanova V, Rodt T, Meyer B, Waldeck S, Wacker F, et al. Influence of sinogram affirmed iterative reconstruction of CT data on image noise characteristics and low-contrast detectability: an objective approach. PLoS One 2013;8(2):e56875.
[13] Nakaura T, Nakamura S, Maruyama N, Funama Y, Awai K, Harada K, et al. Low contrast agent and radiation dose protocol for hepatic dynamic CT of thin adults at 256-detector row CT: effect of low tube voltage and hybrid iterative reconstruction algorithm on image quality. Radiology 2012;264(2):445—54.
[14] Kalra MK, Woisetschlager M, Dahlstrom N, Singh S, Lindblom M, Choy G, et al. Radiation dose reduction with Sinogram Affirmed Iterative Reconstruction technique for abdominal computed tomography. J Comput Assist Tomogr 2012;36(3):339—46.
[15] Schulz B, Beeres M, Bodelle B, Bauer R, Al-Butmeh F, Thalhammer A, et al. Performance of iterative image reconstruction in CT of the paranasal sinuses: a phantom study. AJNR Am J Neuroradiol 2013;34(5):1072—6.
[16] Greffier J, Fernandez A, Macri F, Freitag C, Metge L, Beregi JP. Which dose for what image? Iterative reconstruction for CT scan. Diagn Interv Imaging 2013;94(11):1117—21.
[17] Burckel LA, Defez D, Chaillot PF, Douek P, Boussel L. Use of an automatic recording system for CT doses: Evaluation of the impact of iterative reconstruction on radiation exposure in clinical practice. Diagn Interv Imaging 2015;96(1):265—72, http://dx.doi.org/10.1016/j.diii.2014.11.014.
[18] Gervaise A, Osemont B, Louis M, Lecocq S, Teixeira P, Blum A. Standard dose versus low-dose abdominal and pelvic CT: comparison between filtered back projection versus adaptive iterative dose reduction 3D. Diagn Interv Imaging 2014;95:47—53.
[19] Gervaise A, Teixeira P, Villani N, Lecocq S, Louis M, Blum A. CT dose optimisation and reduction in osteoarticular disease. Diagn Interv Imaging 2013;94:371—88.
[20] Baumueller S, Winklehner A, Karlo C, Goetti R, Flohr T, Russi EW, et al. Low-dose CT of the lung: potential value of iterative reconstructions. Eur Radiol 2012;22(12):2597—606.
[21] Mieville FA, Gudinchet F, Brunelle F, Bochud FO, Verdun FR. Iterative reconstruction methods in two different MDCT scanners: physical metrics and 4-alternative forced-choice detectability experiments—a phantom approach. Phys Med 2013;29(1):99—110.
[22] Mieville F, Beaumont S, Torfeh T, Gudinchet F, Verdun FR. Computed tomography commissioning programmes: how to obtain a reliable MTF with an automatic approach? Radiat Prot Dosimetry 2010;139(1—3):443—8.
[23] Richard S, Husarik DB, Yadava G, Murphy SN, Samei E. Towards task-based assessment of CT performance: system and object MTF across different reconstruction algorithms. Med Phys 2012;39(7):4115—22.
[24] Ghetti C, Palleri F, Serreli G, Ortenzia O, Ruffini L. Physical characterization of a new CT iterative reconstruction method operating in sinogram space. J Appl Clin Med Phys 2013;14(4):4347.
[25] Boedeker KL, McNitt-Gray MF. Application of the noise power spectrum in modern diagnostic MDCT: part II. Noise power spectra and signal to noise. Phys Med Biol 2007;52(14):4047—61.
[26] Solomon JB, Christianson O, Samei E. Quantitative comparison of noise texture across CT scanners from different manufacturers. Med Phys 2012;39(10):6048—55.
[27] Love A, Olsson ML, Siemund R, Stalhammar F, Bjorkman-Burtscher IM, Soderberg M. Six iterative reconstruction algorithms in brain CT: a phantom study on image

quality at different radiation dose levels. Br J Radiol 2013;86(1031):20130388.
[28] Ott JG, Becce F, Monnin P, Schmidt S, Bochud FO, Verdun FR. Update on the non-prewhitening model observer in computed tomography for the assessment of the adaptive statistical and model-based iterative reconstruction algorithms. Phys Med Biol 2014;59(15):4047—64.
[29] Arrêté du 24 octobre 2011 relatif aux niveaux de référence diagnostiques en radiologie et en médecine nucléaire. (J.O.14 janvier 2012).